International Journal of Advanced Information in Engineering Technology (IJAIET) ISSN: 2454-6933
Vol.3, No.3, March 2016

Analysis and Design of an Improved Non-Isolated Bidirectional DC-DC Converter

Sona Xavier
Dept. of Electrical and Electronics
Mangalam College of Engineering
Kottayam, India

Jeepa K.J
Asst. Professor, Dept. of Electrical and Electronics
Mangalam College of Engineering
Kottayam, India

***Abstract*—Bidirectional dc-dc converters (BDC) have recently received a lot of attention due to the increasing need to systems with the capability of bidirectional energy transfer between two dc buses. This paper introduces an improved non-isolated bidirectional DC–DC converter. The proposed converter have wide voltage gain than the conventional and coupled inductor type bidirectional converters in both step-up as well as step-down modes. Therefore the proposed converter can be operated in wide-voltage-conversion range. The voltage stresses on the switches of the proposed converter are a half of the high voltage side. In addition, the operating principle and steady-state analyses are explained. Simulations were carried out in MATLAB/SIMULINK.**

Keywords—*Bidirectional dc-dc converter, Coupled inductor, Non-isolated*

I. Introduction

The bidirectional DC-DC converters are involved in power flow between two dc sources. They allow power flow in both the direction without change in polarity of voltage. They have been widely used in various areas, such as appliances, general industries, and aerospace [1], which include uninterruptible power supplies [2], solar power supplies for satellites, hybrid electric vehicles (EVs) [3], intelligent battery chargers, and power converters for fuel-cell vehicles [4].

The fluctuation nature of most renewable energy resources, like wind and solar, makesthem unsuitable for standalone operation as the sole source of power. A common solutionto overcome this problem is to use an energy storage device besides the renewable energyresource to compensate for these fluctuations and maintain a smooth and continuouspower flow to the load. As the most common and economical energy storage devices inmedium-power range are batteries and super-capacitors, a dc-dc converter is alwaysrequired to allow energy exchange between storage device and the rest of system. Such aconverter must have bidirectional power flow capability with flexible control in alloperating modes [5].

Bidirectional dc-dc converters can be classified into isolated versions and non-isolated versions. It depends on the applications. The big advantage of an isolated bidirectional dc–dc converter is galvanic isolation which is an effective method for breaking a ground loop. However, this converter requires an isolated transformer and more than four switches for galvanic isolation so that its efficiency is lower than that of a non-isolated-type converter.The isolated types includes the flyback type [6], forward-flyback type [7], half-bridge type [4] and full-bridge type [1].On the other hand, the advantages of a non-isolated bidirectional dc–dc converter are simple structure, fundamentally including an inductor and two switches, and higher efficiency than an isolated-type converter. This paper focuses on the non-isolated bidirectional dc-dc converter. The non-isolated types include the multi-level type [8], switched-capacitor type, cuk/cuk type, sepic/zeta type, buck-boost type, coupled-inductor type [9], three-level type and conventional buck/boost type [9], [10]. In these, the circuit structure of the buck-boost type is very simple and can easily implemented. Fig.1 shows the conventional bidirectional buck/boost converter. However, this converter has low step-up and step-down voltage gain and hence it is not suitable for wide voltage-conversion applications.

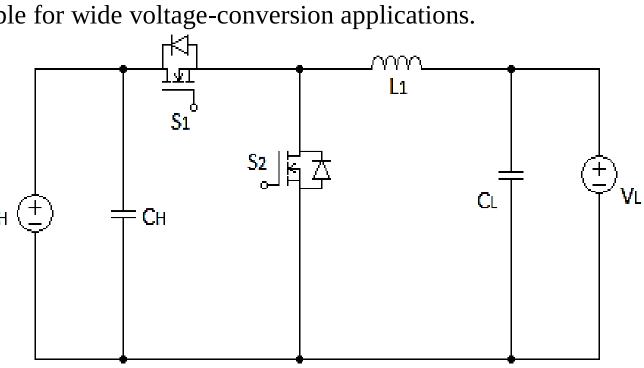

Fig. 1 Conventional bidirectional buck/boost converter

Another conventional type of bidirectional buck/boost converter is the coupled inductor type bidirectional converter which is shown in fig.2. This converter can achieve large voltage gain by adjusting the turn ratio of the coupled inductor. However, the circuit configurations are complicated. Also, this converter does not have wide voltage gain as that of the proposed converter.

An improved non-isolated bidirectional buck/boost converter is shown in fig.3. This converter offers wide voltage gain than the above mentioned conventional topologies. Also, the proposed topology has low voltage stresses across the switches as compared to other two topologies.

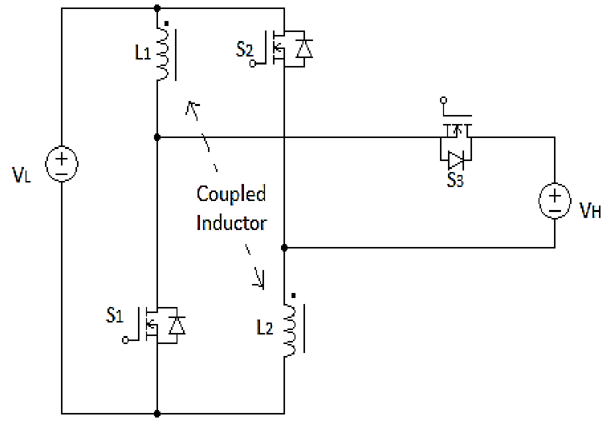

Fig 2. Coupled inductor type bidirectional converter

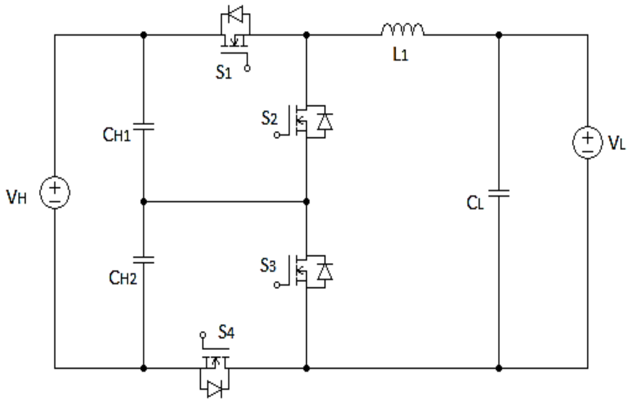

Fig 3. Proposed bidirectional buck/boost converter

The operating principles and steady state analysis in both step-down and step-up modes is described below. The major assumptions to be taken for the analysis are: (i) The ON-state resistance $R_{DS(ON)}$ of the switches and the ESR of the capacitors are ignored. (ii) The capacitors C_{H1}, C_{H2} and C_L are large enough, and voltage across the capacitors can be treated as constant. (iii) The capacitance of the capacitors C_{H1} and C_{H2} are equal. Thus $V_{H1} = V_{H2} = V_{H/2}$

II. STEP-DOWN MODE

The equivalent circuit of the proposed converter in step-down mode is shown in Fig. 4. In this mode the switches S_1 and S_4 are controlled and switches S_2 and S_3 are used as synchronous rectifiers. The typical waveforms in continuous conduction mode (CCM) is shown in Fig 7. The different operational modes are explained as follows:

1. Mode 1$[t_0 - t_1]$: The switches S_1 and S_3 are turned on and the switches S_2 and S_4 are turned off. The switch S_3 is used for the synchronous rectifier. The direction of current flow is shown in fig 5. Here, the energy in the high voltage side is transferred to the inductor L_1, capacitor C_L, and load R_L.

Thus, the voltage across the inductor L_1 is given by

$$v^1{}_{L1} = \frac{v_H}{2} - v_L (1)$$

The current through the inductor L_1 is obtained as

$$i^1{}_{L1}(t) = i_{L1}(t_0) + \frac{1}{L_1}\left(\frac{V_H}{2} - V_L\right)(t - t_0) \qquad (2)$$

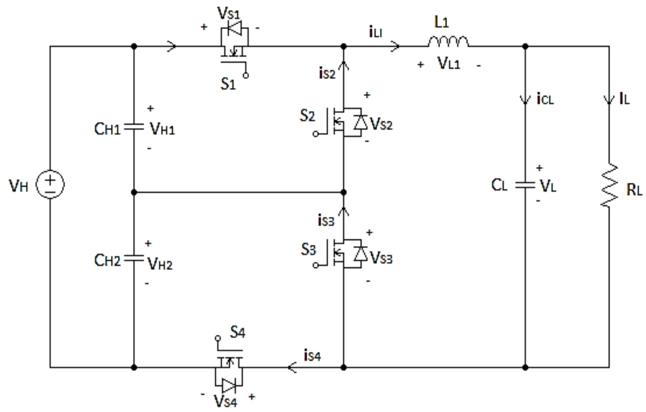

Fig 4. Equivalent circuit of the proposed converter in step-down mode

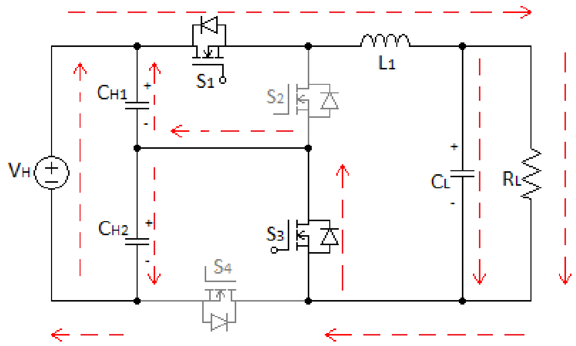

Fig 5. Current flow path of the proposed converter in mode 1

2. Mode 2$[t_1 - t_2]$:The switches S_2 and S_3 are turned on and the switches S_1 and S_4 are turned off. The switches S_2 and S_3 are used for the synchronous rectifiers. The path of current-flow of the converter is shown in fig 6. The stored energy in the inductor L_1 is released to the capacitor C_L and load R_L.

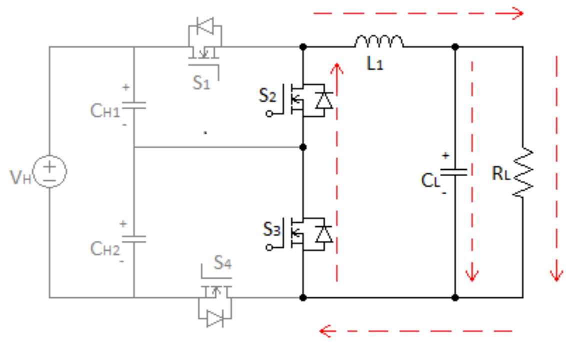

Fig 6. Current flow path of the proposed converter in mode 2

Thus, the voltage across the inductor L1 is found to be

$$v^{11}{}_{L1} = -v_L (3)$$

The current through the inductor L1 is derived as

$$i^{11}{}_{L1}(t) = i_{L1}(t_1) - \frac{V_L}{L_1}(t - t_1) \quad (4)$$

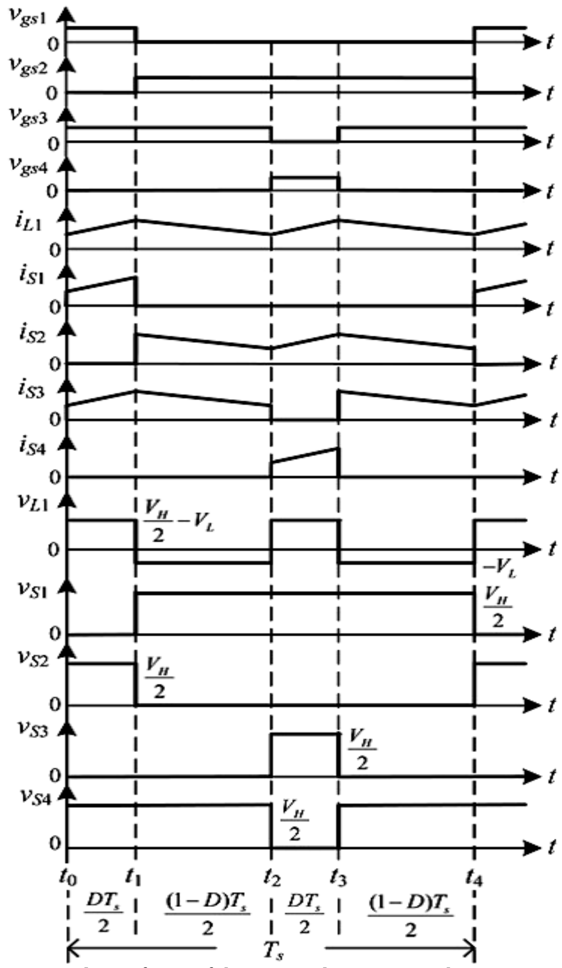

Fig. 7 Typical waveforms of the proposed converter with CCM operation in the step-down mode

*3. Mode 3[t_2 – t_3]:*The switches S_2 and S_4 are turned on and the switches S_1 and S_3 are turned off. And, the switch S_2 is used for the synchronous rectifier. The direction of current-flow of the proposed converter is shown in fig.4.6.

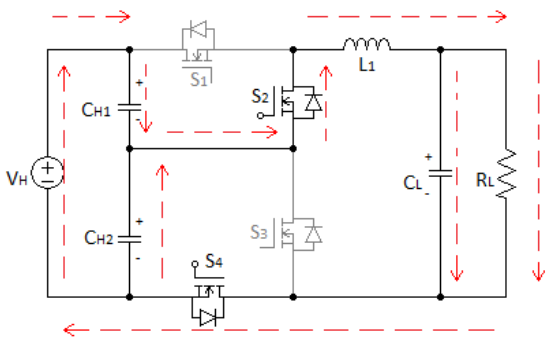

Fig 8. Current flow path of the proposed converter in mode 3

The energy of the high-voltage side V_{H2} is transferred to the inductor L_1, capacitor C_L, and load R_L.

Thus, the voltage across the inductor L_1 is obtained as

$$v^{111}{}_{L1} = \frac{v_H}{2} - v_L (5)$$

The current through the inductor L_1 is given as

$$i^{111}{}_{L1}(t) = i_{L1}(t_2) + \frac{1}{L_1}\left(\frac{V_H}{2} - V_L\right)(t - t_2) \quad (6)$$

*4. Mode 4[t_3 – t_4]:*This operation principle in this mode is the same as the mode 2. Thus, the voltage across the inductor L_1 is determined as follows

$$v^{1V}{}_{L1} = -v_L (7)$$

The current through the inductor L_1 is derived as

$$i^{1V}{}_{L1}(t) = i_{L1}(t_3) - \frac{V_L}{L_1}(t - t_3) (8)$$

By using the volt-sec balance principle on the inductor L_1, it can obtain

$$\int_0^{DT_S/2} V^{1}{}_{L1} dt + \int_0^{\left(\frac{(1-D)T_S}{2}\right)} V^{11}{}_{L1} dt + \int_0^{DT_S/2} V^{111}{}_{L1} dt + \int_0^{((1-D)T_S/2)} V^{1V}{}_{L1} dt = 0 \quad (9)$$

Solving the above integral, the voltage gain obtained is given by

$$M_{step-down} = \frac{V_L}{V_H} = \frac{D}{2} (10)$$

From the boundary-conduction mode (BCM), the following equations can be derived

The normalized inductor time constant τ_{LL} is defined as

$$\tau_{LL} = \frac{L_1}{R_L T_S} = \frac{L_1 f_S}{R_L} (11)$$

Also. The boundary of τ_{LL} is given by

$$\tau_{LLB} = \frac{1-D}{4} (12)$$

III. STEP-UP MODE

The equivalent circuit of the proposed converter in the step-up mode is shown in fig.9. Here, the switches S_2 and $S_3$are controlled and the switches S_1 and S_4 are used for the synchronous rectifiers. The typical waveform in CCM is shown in the Fig 12. The operating principles and steady-state analyses are described as follows:

*1.Mode 1[t_0 – t_1]:*The switches S_2 and S_3 are turned on and the switches S_1 and S_4 are turned off. The current-flow path of the proposed converter is shown in fig.10. The energy of the low-voltage side V_L is transferred to the inductor L_1. The

capacitors C_{H1} and C_{H2} are stacked to discharge for the load R_L.
Thus, the voltage across the inductor L_1 is given by

$$v^1{}_{L1} = v_L \quad (13)$$

The current through the inductor L_1 is derived as

$$i^1{}_{L1}(t) = i_{L1}(t_0) + \frac{V_L}{L_1}(t - t_0) \quad (14)$$

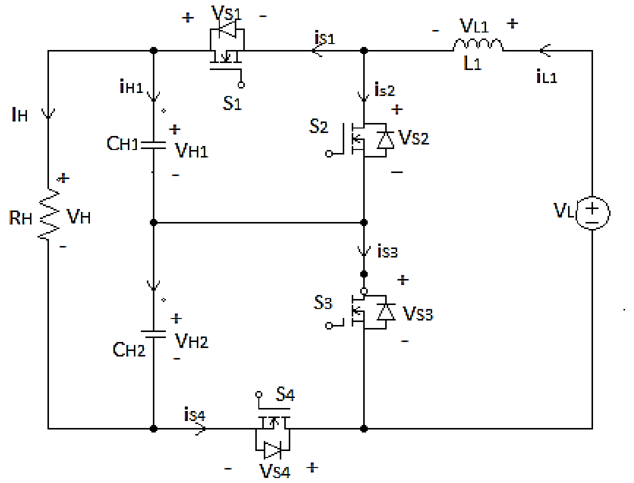

Fig 9. Equivalent circuit of the proposed converter in step-up mode

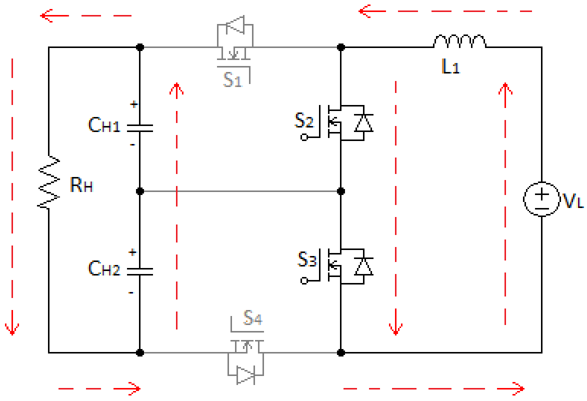

Fig 10. Current flow path of the proposed converter in mode 1

*2. Mode 2[$t_1 - t_2$]:*The switches S_1 and S_3 are turned on and the switches S_2 and S_4 are turned off. And, the switch S_1 is used for the synchronous rectifier. The path of current-flow of the proposed converter is shown in fig.11. The energies of the low-voltage side V_L and inductor L_1 are series to release their energies to the capacitor C_{H1}. The capacitors C_{H1} and C_{H2} are stacked to discharge for the load R_H.
Thus, the voltage across the inductor L_1 is found to be

$$v^{11}{}_{L1} = -\frac{v_H}{2} + v_L \quad (15)$$

The current through the inductor L_1 is given as

$$i^{11}{}_{L1}(t) = i_{L1}(t_1) + \frac{1}{L_1}\left(-\frac{V_H}{2} + V_L\right)(t - t_1) \quad (16)$$

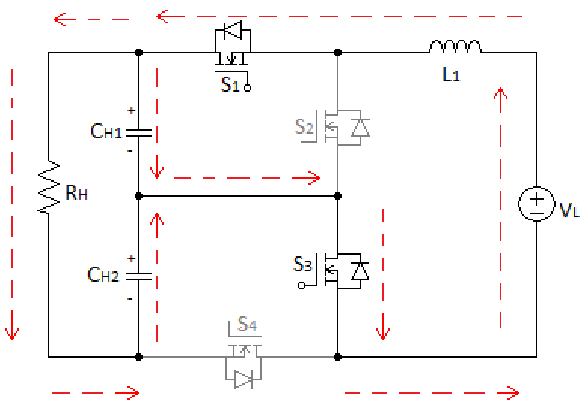

Fig 11. Current flow path of the proposed converter in mode 2

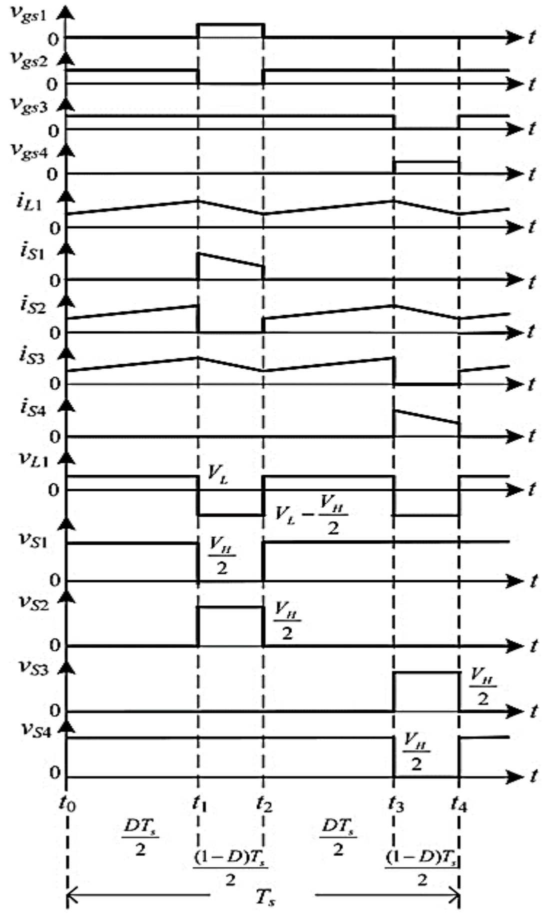

Fig 12.Typical waveforms of the proposed converter with CCM operation in the step-down mode

*3. Mode 3[$t_2 - t_3$]:*The operation principle in this mode is the same as the mode 1. Thus, the voltage across the inductor L_1 is derived as

$$v^{111}{}_{L1} = v_L \quad (17)$$

The current through the inductor L_1 is derived as

$$i^{111}{}_{L1}(t) = i_{L1}(t_2) + \frac{V_L}{L_1}(t - t_2) \quad (18)$$

*4. Mode 4[$t_3 - t_4$]:*The switches S_2 and S_4 are turned on and the switches S_1 and S_3 are turned off. The switch S_4 is used for the synchronous rectifier. The current-flow path of the proposed converter is shown in fig.13. The energies of the low-voltage side V_L and inductor L_1 are series to release their energies to the capacitor C_{H2}. The capacitors C_{H1} and C_{H2} are stacked to discharge for the load R_H.

Thus, the voltage across the inductor L_1 is found to be

$$v^{1V}{}_{L1} = -\frac{v_H}{2} + v_L (19)$$

The current through the inductor L_1 is given as

$$i^{1V}{}_{L1}(t) = i_{L1}(t_3) + \frac{1}{L_1}\left(-\frac{V_H}{2} + V_L\right)(t - t_3) (20)$$

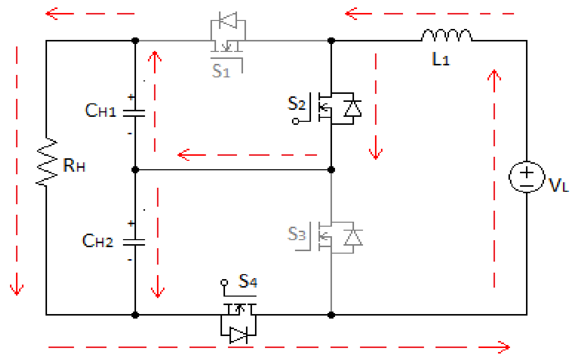

Fig 13. Current flow path of the proposed converter in mode 4

By using the volt-sec balance principle on the inductor L_1, it can obtain

$$\int_0^{DT_S/2} V^{1}{}_{L1}dt + \int_0^{\left(\frac{(1-D)T_S}{2}\right)} V^{11}{}_{L1}dt +$$

$$\int_0^{DT_S/2} V^{111}{}_{L1}dt + \int_0^{((1-D)T_S/2)} V^{1V}{}_{L1}dt = 0 \quad (21)$$

Solving the above integral, the voltage gain obtained is given by

$$M_{step-UP} = \frac{V_H}{V_L} = \frac{2}{1-D} \quad (22)$$

From the boundary-conduction mode (BCM), the following equations can be found out
The normalized inductor time constant τ_{LH} is defined as

$$\tau_{LH} = \frac{L_1}{R_H T_S} = \frac{L_1 f_S}{R_H} (23)$$

Also, the boundary of τ_{LH} is given by

$$\tau_{LHB} = \frac{D(1-D)^2}{16} (24)$$

IV. SIMULATION RESULTS

The circuit model of the proposed bidirectional converter can be implemented and simulated using Matlab/Simulink both in step-down as well as in step-up mode. Figure shows the simulation results of both buck and boost modes. The parameters are chosen as V_H = 200V, V_L = 24V, switching frequency F_s = 50KHz, P_o = 200W, capacitors $C_{H1} = C_{H2} = C_L$ = 100µF, inductor L_1 = 140µH. For the step-down mode the duty cycle can be derived as 0.24 and in step-up mode it is 0.76

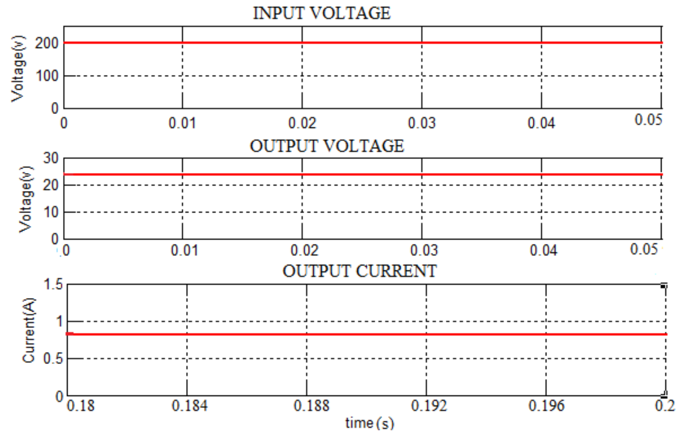

(a)

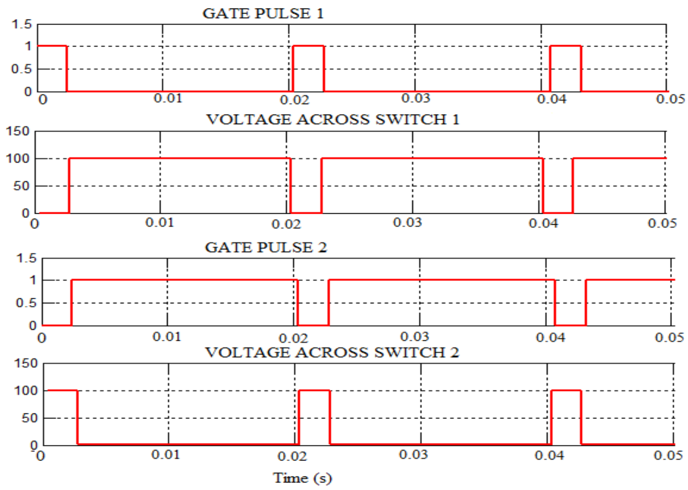

(b)

Fig 15. Simulation waveforms of the proposed converter in the step-down mode

Fig 15 and 16 shows the simulation waveforms of the proposed converter in step-down and step-up mode respectively.The operation of this converter is verified here. From fig 15(a), it can be seen that the low voltage side V_L is well regulated at 24 V and the converter is operated in step-down mode. The waveform of the output current is also shown. From Figs.15 (b) and 16 (b), it is found that the voltage stresses on the switches

S_1 and S_2 are equal to $V_H/2$. Also, it is seen from Fig 16 (a) that the high voltage side V_H is well regulated at 200 V and the converter is operated in step-up mode.

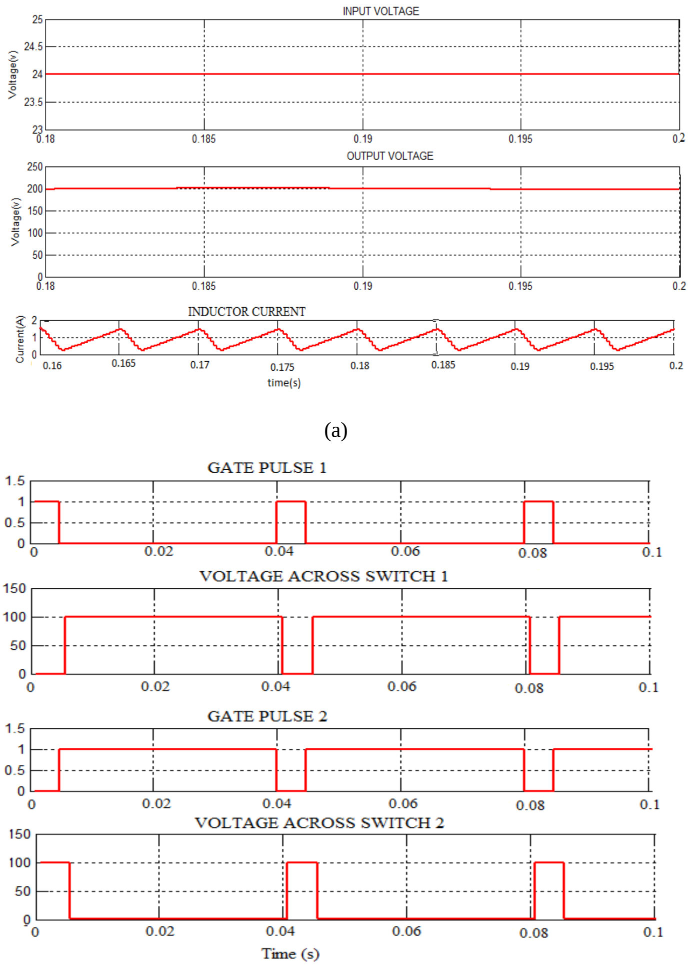

(a)

(b)

Fig 16. Simulation waveforms of the proposed converter in the step-up mode

V. CONCLUSION

This paper presents an improved non-isolated bidirectional buck/boost converter. The circuit configuration of the proposed converter is very simple and it is modified from the conventional buck/boost converter. The proposed converter have wider step-up and step-down voltage gain than the conventional and coupled inductor type buck/boost converter. Also, the voltage stresses on the switches are a half of the high-voltage side. The theoretical analysis and simulation results are provided.

REFERENCES

[1] Naayagi, R.T., Forsyth, A.J., Shuttleworth, R, “High-power bidirectional DC–DC converter for aerospace applications”,IEEE Trans. Power Electron., 2012, 27, (11), pp. 4366–4379.

[2] A. Nasiri, Z. Nie, S. B. Bekiarov, and A. Emadi, “An on-line UPS system with power factor correction and electric isolation using BIFRED converter,” *IEEE Trans. Ind. Electron.*, vol. 55, no. 2, pp. 722–730, Feb. 2008.

[3] M. B. Camara, H. Gualous, F. Gustin, A. Berthon, and B. Dakyo, “DC/DC converter design for supercapacitor and battery power management in hybrid vehicle applications—Polynomial control strategy,” *IEEE Trans. Ind. Electron.*, vol. 57, no. 2, pp. 587–597, Feb. 2010.

[4] F. Z. Peng, H. Li, G. J. Su, and J. S. Lawler, “A new ZVS bidirectional dc–dc converter for fuel cell and battery application,” *IEEE Trans. Power Electron.*, vol. 19, no. 1, pp. 54–65, Jan. 2004.

[5] S. Jalbrzykowski and T. Citko,” A bidirectional dc-dc converter for renewable energy systems”, bulletin of the polish academy of sciences, Technical sciences, vol. 57, no. 4, 2009.

[6] Chen, G., Lee, Y.S., Hui, S.Y.R., Xu, D., Wang, Y.: ‘Actively clamped bidirectional flyback converter’, *IEEE Trans. Ind. Electron.*, 2000, 47, (4), pp. 770–779.

[7] Huber, L., Jovanovic, M.M.: ‘Forward-flyback converter with current-doubler rectifier: analysis, design, and evaluationresults’, *IEEE Trans. Power Electron*., 1999, 14, (1), pp. 184–192.

[8] Peng, F.Z., Zhang, F., Qian, Z.: ‘A magnetic-less DC–DC converter for dual-voltage automotive systems’, *IEEE Trans. Ind*. Appl., 2003, 39, (2), pp. 511–518

[9] Lung-Sheng Yang and Tsorng-Juu Liang, “Analysis and Implementation of a Novel Bidirectional DC-DC Converter”, *IEEEtransactions on industrial electronics*, vol. 59, no. 1, January 2012.

[10] C.-C. Lin, L.-S. Yang, G.W. Wu, “Study of a non-isolated bidirectional DC–DC converter”, *IET Power Electron.*, 2013, Vol. 6, Iss. 1, pp. 30–37 doi: 10.1049/iet-pel.2012.0338.